of a carbonyl oxygen was observed before by Gold for 2,6-dimethylpyrone.[8,9]

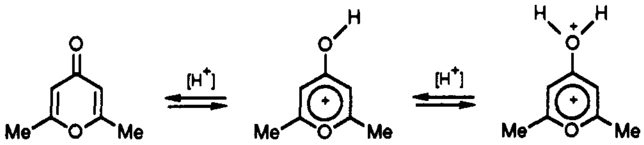

The half-life for the overall reaction of 5 (isomerization, dehydrogenation, and cracking) initiated by formation of 6 in 1:1 FSO_3H-SbF_5 was determined as 630 s at 58.5 °C[3b]. As we observed no conversion of 4 in the time needed for 60% exchange, the rate-determining step in the conversion must occur after the relatively slow hydronation at C(3). This representation is at variance with the earlier view that the dication once formed rearranges rapidly.[3b]

Experimental Section

All manipulations of superacids and the preparation of samples were conducted in a dry box. A. R. chemicals were used throughout. Mesityl oxide was dried on molecular sieves. Anhydrous trifluoromethanesulfonic acid was prepared by mixing the commercial (98%) acid with its anhydride and allowing several days for the reactions in a stoppered flask warmed occasionally with a hot air blower. Commercial 4:1 FSO_3H-SbF_5 was used as received. FSO_3D and SbF_5 were mixed in equimolar amounts. For the exchange experiments, 12 mmol of this composite acid was diluted with 1.5 mL of $ClSO_2F$ and cooled in dry ice, and a solution of 2.6 mmol of 4 in 1.5 mL of $ClSO_2F$ was added from a capillary funnel, also cooled with dry ice. The pipets used to transfer the samples to the NMR tubes were cooled in liquid nitrogen before use.

The NMR experiments were conducted as described.[2d] The linearity of the $\Delta\delta$ vs concentration plot in H_2SO_4 was checked for 0.05–1 M 4 in solution and found to be very good ($r > 0.998$, except in 55% H_2SO_4, where $r = 0.996$).

Acknowledgment. We are grateful to Exxon Education Foundation for financial support.

Registry No. 4, 141-79-7; 4·H^+, 77406-39-4; 6, 135584-29-1; 7, 135584-28-0.

---

[8] Gold, V.; Mah, T. *J. Chem. Soc., Perkin Trans. 2* **1981**, *812*.

[9] After completion of this work it has been reported that trifluoromethanesulfonic acid catalyzed alkylation of benzene with 3-phenyl-2-propen-1-ones is accelerated upon addition of SbF_5. A second protonation at oxygen was postulated to account for this effect: Ohwada, T.; Yamagata, N.; Shudo, K. *J. Am. Chem. Soc.* **1991**, *113*, 1364.

Proton Affinities and Gas-Phase Basicities of Alkyl and Silyl Ethers

James F. Blake and William L. Jorgensen*

Department of Chemistry, Yale University, New Haven, Connecticut 06511-8118

Received May 7, 1991

The absolute proton affinities and gas-phase basicities for a series of related alkyl and silyl ethers, $(SiH_3)_2O$, H_3SiOCH_3, $(CH_3)_2O$, $H_3SiOSiH_2CH_3$, $H_3COSiH_2CH_3$, $H_3SiOC_2H_5$, $H_3COC_2H_5$, $H_3SiOC(CH_3)_3$, $H_3COSi(CH_3)_3$, and $H_3COC(CH_3)_3$, have been computed via ab initio molecular orbital calculations. Geometry optimizations were carried out at the Hartree–Fock level with the 3-21G and 6-31G(d) basis sets, and correlation energies were computed with second- and third-order Møller–Plesset theory. Vibrational energy changes were also included from 3-21G calculations. It is found that the range of proton affinities spans from 187 to 205 kcal mol^{-1}. Comparisons with available experimental data indicate that the predicted thermodynamic results are accurate to within 3 kcal mol^{-1}. The low gas-phase basicity of disiloxanes is confirmed, while the similar results for dialkyl ethers and analogous alkyl silyl ethers are particularly notable. The structures of the protonated molecules are also characterized in detail.

Introduction

In a previous study,[1] the low oxygen basicity of disiloxanes (disilyl ethers) relative to dialkyl ethers was rationalized by examining highest occupied molecular orbitals (HOMO). Ab initio molecular orbital calculations revealed lower energies and smaller oxygen components for the HOMO of disiloxanes that could explain the observed diminished basicity.[2-6] The relative basicity of the intermediate case, alkyl silyl ethers, is less certain. Despite widespread use of organosilicon compounds in organic chemistry, many thermodynamic data, including proton affinities, remain essentially qualitative.[6,7] Additionally, there are no experimental structures available for protonated alkyl or silyl ethers.

The most accurate methods of determining relative proton affinities involve measurements of gas-phase equilibrium constants for proton-transfer reactions with bases of similar strength using either ion cyclotron resonance (ICR) or high-pressure mass spectroscopy (HPMS).[8] Combined with heats of formation, relative proton affinities can be "anchored", yielding absolute proton affinities for use in thermodynamic cycles. However, equilibrium methods are often problematic for compounds containing silyl groups. The tendency to undergo fragmentation rather than proton transfer often precludes an accurate measurement of the proton affinity.[6,9-12] Through de-

---

[1] Shambayati, S.; Blake, J. F.; Wierschke, S. G.; Jorgensen, W. L.; Schreiber, S. L. *J. Am. Chem. Soc.* **1990**, *112*, 697.

[2] Varma, R.; MacDiarmid, A. G.; Miller, G. *Inorg. Chem.* **1964**, *3*, 1754. Sternbach, B.; MacDiarmid, A. G. *J. Am. Chem. Soc.* **1961**, *83*, 3384.

[3] Keck, G. E.; Castellino, S. *Tetrahedron Lett.* **1987**, *28*, 281. Keck, G. E.; Boden, E. P. *Tetrahedron Lett.* **1984**, *25*, 265.

[4] West, R.; Wilson, L. S.; Powell, D. L. *J. Organomet. Chem.* **1979**, *178*, 5.

[5] Sauer, J. *Z. Chem.* **1982**, *22*, 60.

[6] Pitt, C. G.; Bursey, M. M.; Chatfield, D. A. *J. Chem. Soc., Perkin Trans. 2* **1976**, 434.

[7] Lias, S. G.; Liebman, J. F.; Levin, R. D. *J. Phys. Chem. Ref. Data* **1984**, *13*, 695.

[8] Aue, D. H.; Bowers, M. T. In *Gas Phase Ion Chemistry*; Bowers, M. T., Ed.; Academic Press: New York, 1979; Vol. 2, p 1.

[9] Shea, K. J.; Gobeille, R.; Bramblett, J.; Thompson, E. *J. Am. Chem. Soc.* **1978**, *100*, 1611.

[10] Li, X.; Stone, J. A. *Can. J. Chem.* **1987**, *65*, 2454.

0022-3263/91/1956-6052$02.50/0

Table I. Calculated Total Energies (Hartrees)[a]

species	3-21G	6-31G(d)	MP2	MP3
$(SiH_3)_2O$	652.791 091 3	656.259 021 0	656.590 179 6	656.615 292 4
$(SiH_3)_2OH^+$	653.112 351 4	656.561 197 8	656.891 563 2	656.920 873 7
$H_3SiOSiH_2CH_3$	691.636 028 6	695.309 329 0	695.772 600 7	695.807 790 7
$H_3SiO(H)SiH_2CH_3{}^+$	691.962 960 0	695.618 435 6	696.081 955 9	696.120 428 8
H_3SiOCH_3	402.991 087 5	405.154 845 8	405.540 041 3	405.564 781 7
$H_3SiO(H)CH_3{}^+$	403.332 622 8	405.470 285 3	405.850 212 6	405.878 865 3
$(CH_3)_2O$	153.213 208 0	154.064 745 1	154.502 068 6	154.526 826 5
$(CH_3)_2OH^+$	153.559 595 9	154.382 376 0	154.813 148 3	154.840 979 2
$H_3SiOC_2H_5$	441.816 161 0	444.195 418 6	444.711 666 4	444.745 802 1
$H_3SiO(H)C_2H_5{}^+$	442.162 378 0	444.515 889 0	445.026 524 3	445.064 755 0
$H_3COC_2H_5$	192.037 548 7	193.104 871 3	193.673 048 5	193.707 276 6
$H_3CO(H)C_2H_5{}^+$	192.382 992 5	193.428 575 6	193.990 159 2	194.027 604 9
$H_3COSiH_2CH_3$	441.835 964 8	444.205 263 7	444.722 014 0	444.756 895 1
$H_3CO(H)SiH_2CH_3{}^+$	442.183 384 9	444.527 972 7	445.040 151 5	445.078 915 8
$H_3SiOC(CH_3)_3$	519.464 952 2	522.269 755 5	523.054 830 1	523.106 267 4
$H_3SiO(H)C(CH_3)_3{}^+$	519.818 835 7	522.600 129 1	523.378 808 1	523.434 549 3
$H_3COSi(CH_3)_3$	519.527 191 7	522.302 593 4	523.085 136 9	523.139 761 0
$H_3CO(H)Si(CH_3)_3{}^+$	519.882 158 8	522.637 792 6	523.416 314 0	523.474 827 6
$H_3COC(CH_3)_3$	269.683 378 0	271.175 632 4	272.013 152 2	272.064 618 8
$H_3CO(H)C(CH_3)_3{}^+$	270.039 104 2	271.512 232 8	272.341 906 5	272.400 231 1

[a] Negative of total energies are given. 3-21G energies are reported for 3-21G optimized geometries. 6-31G(d) and correlated energies computed from 6-31G(d) optimized geometries.

termination of the preferred direction of proton transfer, ICR bracketing studies have established the general ordering of gas-phase basicities as $R_3COCR_3 > R_3SiOCR_3 \gg R_3SiOSiR_3$.[6] Not surprisingly, decreasing the number and/or size of the alkyl substituents leads to decreased gas-phase basicity. This ranking has also been obtained in solution-phase studies. For example, analyses of OH stretching frequency shifts for hydrogen bonding with phenol in CCl_4 yielded the basicity order $Me_3COCMe_3 > Me_3SiOCMe_3 \gg Me_3SiOSiMe_3$.[4] Furthermore, earlier results established that CH_3OSiH_3 is a weaker Lewis base toward diborane than CH_3OCH_3.[2]

The focus of our prior study was the geometries of unprotonated silyl ethers including the origin of the wide Si–O–Si and Si–O–C angles.[1] This work has been extended, as reported here, to the calculation of absolute proton affinities and gas-phase basicities for a series of related alkyl and silyl ethers. The results augment the limited experimental data on these systems and provide structures for the protonated species. The specific molecules that have been studied are $(SiH_3)_2O$, H_3SiOCH_3, $(CH_3)_2O$, $H_3SiOSiH_2CH_3$, $H_3COSiH_2CH_3$, $H_3SiOC_2H_5$, $H_3COC_2H_5$, $H_3SiOC(CH_3)_3$, $H_3COSi(CH_3)_3$, $H_3COC(CH_3)_3$, and their protonated forms.

Computational Methods

The ab initio molecular orbital calculations were carried out with the GAUSSIAN 86/88 series of programs on computers in our laboratory.[13] Geometries for all structures were fully optimized by means of analytical energy gradients[14] at the restricted Hartree–Fock (RHF) level of theory with the split-valence 3-21G[15] and 6-31G(d)[16] basis sets; the latter includes a set of d-orbitals on all non-hydrogen atoms. Basis sets with such polarization functions on heavy atoms are well-known to be important for the calculation of accurate proton affinities.[17-20] Electron correlation energies were computed via second- and third-order Møller–Plesset perturbation theory with the 6-31G(d) basis set (MP3/MP2/6-31G(d)//6-31G(d)); the frozen-core approximation was employed.[21] This level of theory is comparable to configuration interaction with full double excitations for the noncore MO's.

Zero-point vibrational energies and their thermal corrections were also computed by scaling the vibrational frequencies[22] obtained with the 3-21G basis set and analytical second derivatives of the energy with respect to nuclear coordinates.[23] Scaled vibrational frequencies below 500 cm^{-1} were treated as classical rotations (i.e., $E^{\mathrm{vib}} = RT/2$).[17] Generally, unscaled frequencies at the 3-21G level are ca. 10–15% too high when compared to experiment, as discussed in detail elsewhere.[22]

Results and Discussion

Geometries. For the unprotonated species, all geometrical variables were optimized within the single constraint of C_s symmetry, as defined by the plane of the heavy-atom skeleton. The only exceptions were for dimethyl ether (C_{2v}), disiloxane (C_{2v}), and *tert*-butyl silyl ether (C_1). The protonated species were fully optimized with no symmetry constraints (i.e., C_1). The 6-31G(d) structures obtained from these optimizations are illustrated in Figures 1–5. Vibrational analysis verified the location of true minima for the 3-21G optimized structures. The 6-31G(d) optimizations were carried out utilizing the computed 3-21G force constants as an initial guess for the Hessian matrix.

---

(11) Stone, J. A.; Wojtyniak, A. C. M.; Wytenburg, W. *Can. J. Chem.* **1986**, *64*, 575.

(12) Wojtyniak, A. C. M.; Stone, J. A. *Int. J. Mass Spectrom. Ion Processes* **1986**, *74*, 59. Li, X.; Stone, J. A. *Can. J. Chem.* **1988**, *66*, 1288.

(13) Frisch, M. J.; Binkley, J. S.; Schlegel, H. B.; Raghavachari, K.; Melius, C. F.; Martin, R. L.; Stewart, J. J. P.; Bobrowicz, F. W.; Rohlfing, C. M.; Kahn, L. R.; DeFrees, D. J.; Seeger, R.; Whiteside, R. A.; Fox, D. J.; Fluder, E. M.; Pople, J. A. *Gaussian 86*; Gaussian, Inc.: Pittsburgh, PA 15213. Frisch, M. J.; Head-Gordon, M.; Schlegel, H. B.; Raghavachari, K.; Binkley, J. S.; Gonzalez, C.; DeFrees, D. J.; Fox, D. J.; Whiteside, R. A.; Seeger, R.; Melius, C. F.; Baker, J.; Kahn, L. R.; Stewart, J. J. P.; Fluder, E. M.; Topiol, S.; Pople, J. A. *Gaussian 88*; Gaussian, Inc.: Pittsburgh, PA 15213.

(14) Schlegel, H. B. *J. Comput. Chem.* **1982**, *3*, 214.

(15) Binkley, J. S.; Pople, J. A.; Hehre, W. J. *J. Am. Chem. Soc.* **1980**, *102*, 939. Gordon, M. S.; Binkley, J. S.; Pople, J. A.; Pietro, W. J.; Hehre, W. J. *J. Am. Chem. Soc.* **1982**, *104*, 2797.

(16) Hariharan, P. C.; Pople, J. A. *Theor. Chim. Acta* **1973**, *28*, 213. Francl, M. M.; Pietro, W. J.; Hehre, W. J.; Binkley, J. S.; Gordon, M. S.; DeFrees, D. J.; Pople, J. A. *J. Chem. Phys.* **1982**, *77*, 3654.

(17) Hehre, W. J.; Radom, L.; Schleyer, P. v. R.; Pople, J. A. *Ab Initio Molecular Orbital Theory*; Wiley: New York, 1986.

(18) (a) Glidewell, C.; Thomson, C. *J. Comput. Chem.* **1982**, *3*, 495. (b) Hendewerk, M. L.; Frey, R.; Dixon, D. A. *J. Phys. Chem.* **1983**, *87*, 2026.

(19) Frisch, M. J.; Del Bene, J. E.; Raghavachari, K.; Pople, J. A. *Chem. Phys. Lett.* **1981**, *83*, 240.

(20) Del Bene, J. E. *J. Comput. Chem.* **1985**, *6*, 296.

(21) Møller, C.; Plesset, M. S. *Phys. Rev.* **1934**, *46*, 618. Pople, J. A.; Seeger, R.; Krishnan, R. *Int. J. Quant. Chem., Quantum Chem. Symp.* **1977**, *11*, 149.

(22) A scale factor of 0.89 was used: Pople, J. A.; Schlegel, H. B.; Krishnan, R.; DeFrees, D. J.; Binkley, J. S.; Frisch, M. J.; Whiteside, R. A.; Hout, R. F., Jr.; Hehre, W. J. *Int. J. Quantum Chem., Quantum Chem. Symp.* **1981**, *15*, 269.

(23) Pople, J. A.; Krishnan, R.; Schlegel, H. B.; Binkley, J. S. *Int. J. Quantum Chem., Quantum Chem. Symp.* **1979**, *13*, 225.

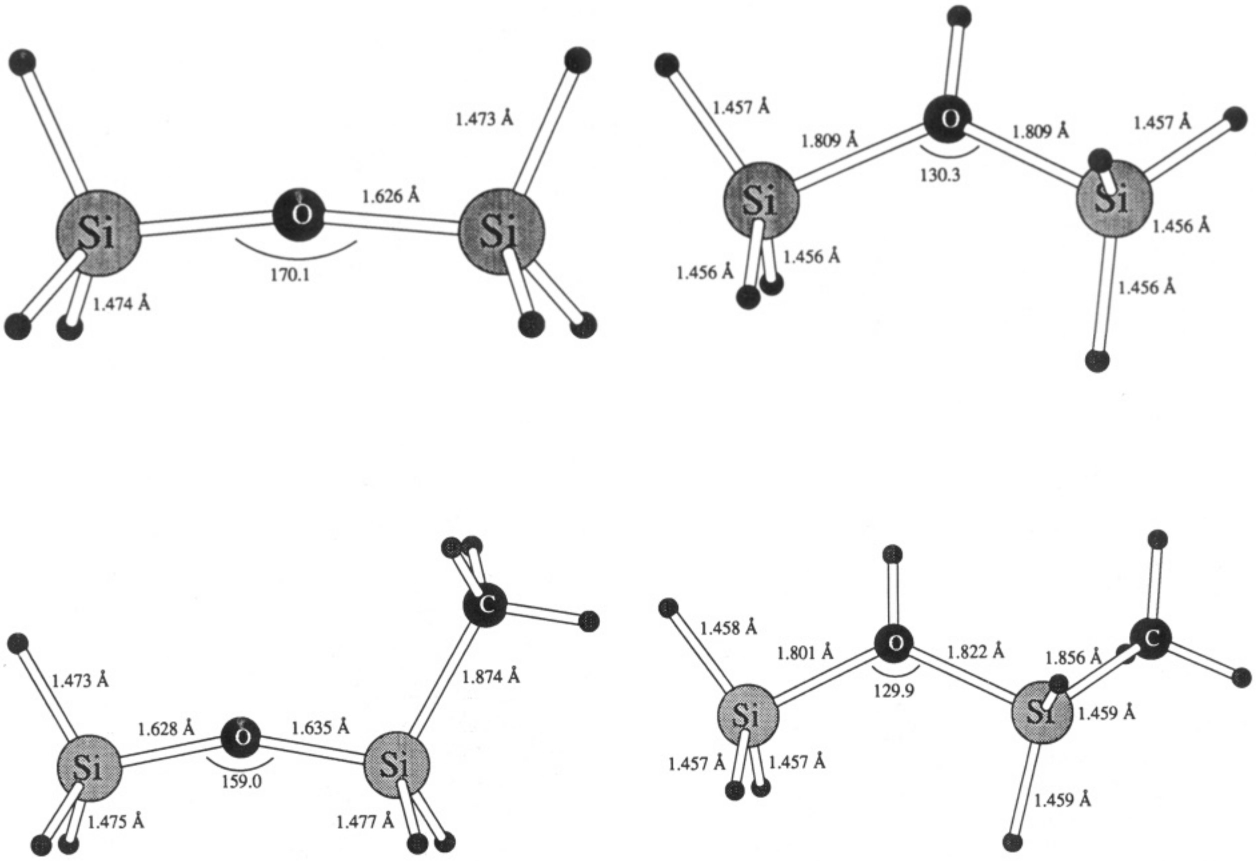

Figure 1. Optimized structures for disiloxane (top) and methyl disiloxane (bottom) from 6-31G(d) calculations.

This proved to be an efficient procedure for the determination of the structures at the higher level. Frequency analysis was not performed on the 6-31G(d) structures due to the imposing computational demands. However, confidence that the optimized geometries represent true stationary points comes in part from the exhibited similarities to the 3-21G structures. Total RMS deviations between the 3-21G and 6-31G(d) structures are less than 0.2 Å, with most deviations less than ca. 0.08 Å. Generally, geometries obtained with the 6-31G(d) basis set are highly accurate.[17] Total energies for the neutral and protonated structures are recorded in Table I.

The geometries of dimethyl ether, methoxysilane, disiloxane, *tert*-butyl silyl ether, and methyl trimethylsilyl ether have been discussed previously.[1] The only significant difference found here is the existence of an imaginary frequency in the previously reported C_s-constrained structure for *tert*-butyl silyl ether (vide infra).

Comparison of the neutral and protonated forms of disiloxane (Figure 1) is distorted by the overestimate of the Si–O–Si bond angle in disiloxane at the 6-31G(d) level (170.1° vs 144.1° from experiment[24]). This is a remarkably soft angle with an inversion barrier of only 0.3–0.4 kcal mol^{-1}.[1] On the basis of our earlier computations, it is reasonable to assume that the discrepancies between theory and experiment would be eliminated if correlated geometries were obtained. Nevertheless, the computed O–Si bond length in disiloxane of 1.626 Å agrees well with the experimental value of 1.634 Å[24] and upon protonation is computed to lengthen considerably to 1.809 Å. For all species considered, O–Si bonds lengthen by an average of 0.178 Å upon protonation. Methyl disiloxane (Figure 1) similarly displays a wide Si–O–Si bond angle as in disiloxane, though diminished by 11.1° to 159.0° at the 6-31G(d) level. The $O{-}SiH_2CH_3$ bond length (1.635 Å) is calculated to be 0.007 Å longer than the $O{-}SiH_3$ bond. For comparison, the O–Si bond length, observed from gas-phase electron diffraction studies, in hexamethyldisiloxane (HMDS) is 1.631 ± 0.003 Å, r(Si–C) = 1.865 ± 0.004 Å, and ∠ Si–O–Si = 148 ± 3°.[25] One should expect the computed Si–O–Si bond angle in methyldisiloxane to be overestimated at the 6-31G(d) level of theory, as for disiloxane. Experimental uncertainties may also be significant; reported values for Si–O–Si bond angles range from 128 to 155° in a variety of compounds.[26] Upon protonation, the $O{-}SiH_3$ bond in methyl disiloxane is calculated to lengthen by 0.173 Å, while the $O{-}SiH_2CH_3$ bond lengthens by a somewhat larger amount, 0.187 Å.

Methoxysilane is the simplest alkoxysilane, and the salient features of protonation are illustrated well in this example. The computed value for the Si–O–C angle in methoxysilane (125.0°) now agrees reasonably with the observed value of 120.6°.[27] The computed $O{-}SiH_3$ bond length is also exactly correct at the 6-31G(d) level of theory, while the O–C bond is predicted to be 0.018 Å too short.[27] As illustrated in Figure 2, the Si–O–C angle increases by 2° upon protonation. This is accompanied by increases in the O–C and O–Si bond lengths of 0.080 and 0.174 Å, respectively. Overall, the average Si–O–C angle widening of alkoxysilanes is 1.9° upon protonation. Note that this average does not include the decrease in the C–O–Si bond angle of *tert*-butyl silyl ether (TBSE) that is discussed below. Otherwise, these changes in geometrical parameters

---

(24) Almenningen, A.; Bastiansen, O.; Hedberg, K.; Traetteberg, M. *Acta Chem. Scand.* **1963**, *17*, 2455.

(25) Csákvári, B.; Wagner, Zs.; Gömöry, P.; Mijlhoff, F. C.; Rozsondai, B.; Hargittai, I. *J. Organomet. Chem.* **1976**, *107*, 287.

(26) Oberhammer, H.; Zeil, W.; Fogarasi, G. *J. Mol. Struct.* **1973**, *18*, 309.

(27) Glidwell, C.; Rankin, D. W. H.; Robiette, A. G.; Sheldrick, G. M.; Beagly, B.; Freeman, J. M. *J. Mol. Struct.* **1970**, *5*, 417.

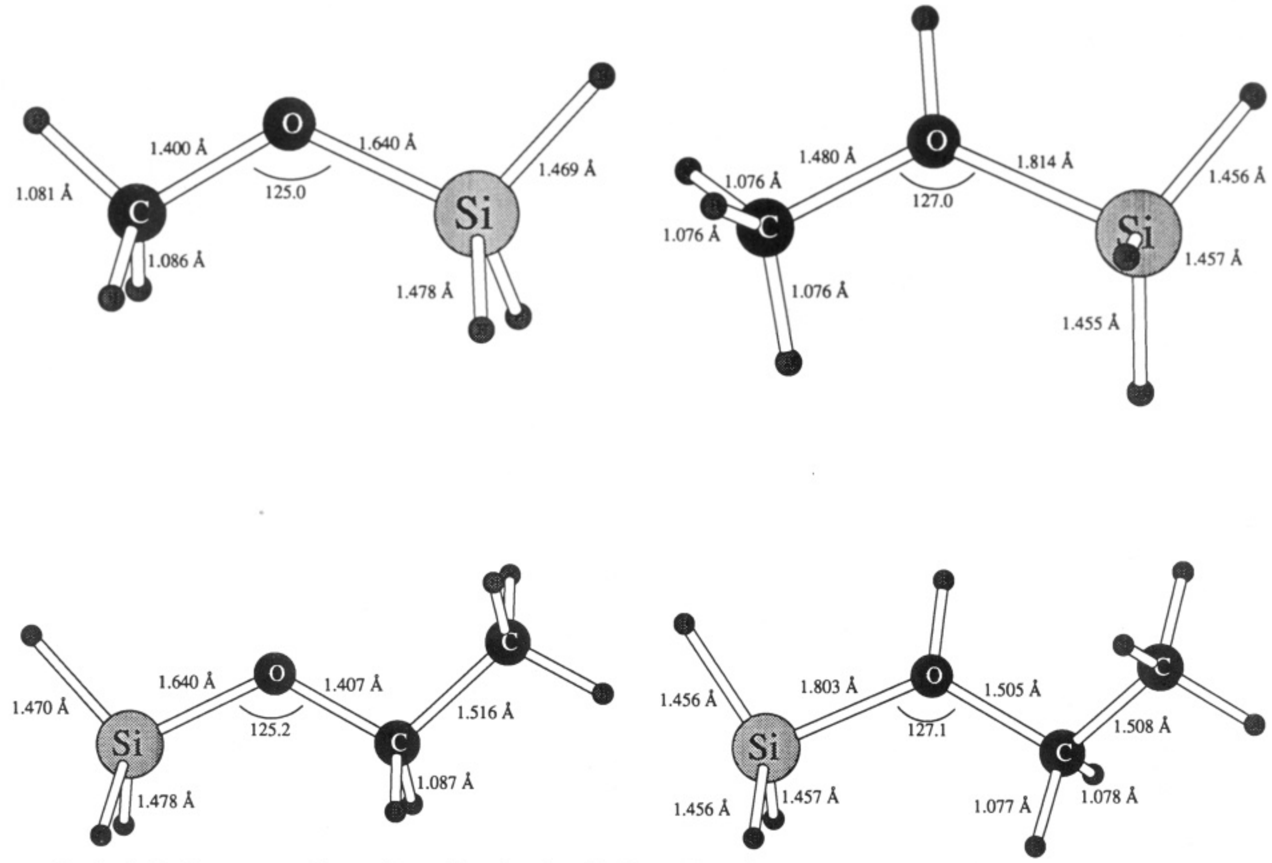

Figure 2. Optimized structures for methoxysilane (top) and ethoxysilane (bottom) from 6-31G(d) calculations.

can be seen as a general feature of the protonation reactions.

Replacement of the methyl group in methoxysilane by an ethyl group (Figure 2), causes minor effects for the majority of geometrical parameters. The O–Si bond length remains the same as in methoxysilane, while the O–C bond lengthens by only 0.007 Å. Likewise, upon protonation ethoxysilane reflects much of the same character as protonated methoxysilane. The Si–O–C angle increases to 127.1°. The O–Si bond increases by 0.163 Å, 0.011 Å less than the O–Si increase in methoxysilane. The O–C distance increases by 0.098 Å, a slightly greater increase (0.018 Å) than in methoxysilane. Interestingly, the C–C distance decreases upon protonation by 0.008 Å. In fact, in all the protonated structures, all bonds to the atoms adjacent to the protonated oxygen shorten except for the bonds to the oxygen. This reflects a change towards sp^2 hybridization at these atoms consistent with contributions from the dissociated resonance structures:

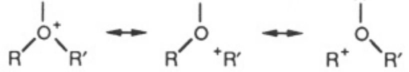

As the ability of the adjacent atoms to stabilize the positive charge increases, the bonds to oxygen lengthen and the other bonds to the adjacent atoms shorten.

Further replacement of the ethyl group by *tert*-butyl gives rise to understandable geometrical perturbations (Figure 3, top). As stated above, the C_s structure previously reported for TBSE is not a minimum; the negative force constant in the Hessian matrix corresponds to small rotations of the silyl (11.7°) and *tert*-butyl groups (17.3°) in comparison to the C_s structure. Relaxing the symmetry constraint lowers the total energy by ca. 0.1 kcal mol^{-1} and affords minor changes in other geometrical parameters (cf. Figure 3 and Figure 14 in ref 1). The extension of the O–Si bond (0.148 Å) upon protonation is similar to the 0.163 Å for ethoxysilane. However, the extension of the O–C bond by 0.160 Å for the *tert*-butyl substituent is now much greater than the 0.098 Å for the ethyl group. This reflects the greater stability of the tertiary carbocation component in the resonance structures over the primary one and is further evidenced by the 0.011 Å shortening of the C_α–C_β bonds in $H_3SiO(H)C(CH_3)_3^+$ as compared to the 0.008 Å shortening in $H_3SiO(H)CH_2CH_3^+$. Curiously, the protonation of TBSE leads to the only predicted decrease in an X–O–Y angle among the compounds studied here. Though the effect is small, a possible explanation can be offered. In view of the resonance structure analysis, the protonated molecule has significant silanol–*tert*-butyl cation character. For silanol itself, the computed Si–O–H angle is wide (120–130°),[28] which would tend to compress the other angles at oxygen in protonated TBSE.

Turning to the alkylation of the silyl group in methoxysilane, the results for methyl methylsilyl ether (MMSE) are shown at the bottom of Figure 3. As in the case of ethyl silyl ether, the geometry of the CH_2OSiH_2 unit in MMSE differs little from that in methoxysilane. Protonation exerts the now familiar distortions upon MMSE. The lengths of the O–C and O–Si bonds increase by 0.076 and 0.185 Å, respectively, while the C–O–Si bond angle increases by 1.5°. As in methyl disiloxane, the C–Si bond decreases by 0.018 Å. Methyl trimethylsilyl ether (MTMSE) was then the next computational target in the alkylated silyl series (Figure 4). The C–O–Si bond angle in MTMSE is predicted to be a little wider (2.2°) than in methoxysilane. The O–Si bond is 0.014 Å longer, and the O–C bond length is decreased by 0.004 Å. In comparison

---

[28] Kahn, S. D.; Keck, G. E.; Hehre, W. J. *Tetrahedron Lett.* **1987**, *28*, 279. Schleyer, P. v. R. *Pure Appl. Chem.* **1987**, *59*, 1647. Laird, E. R. Unpublished results.

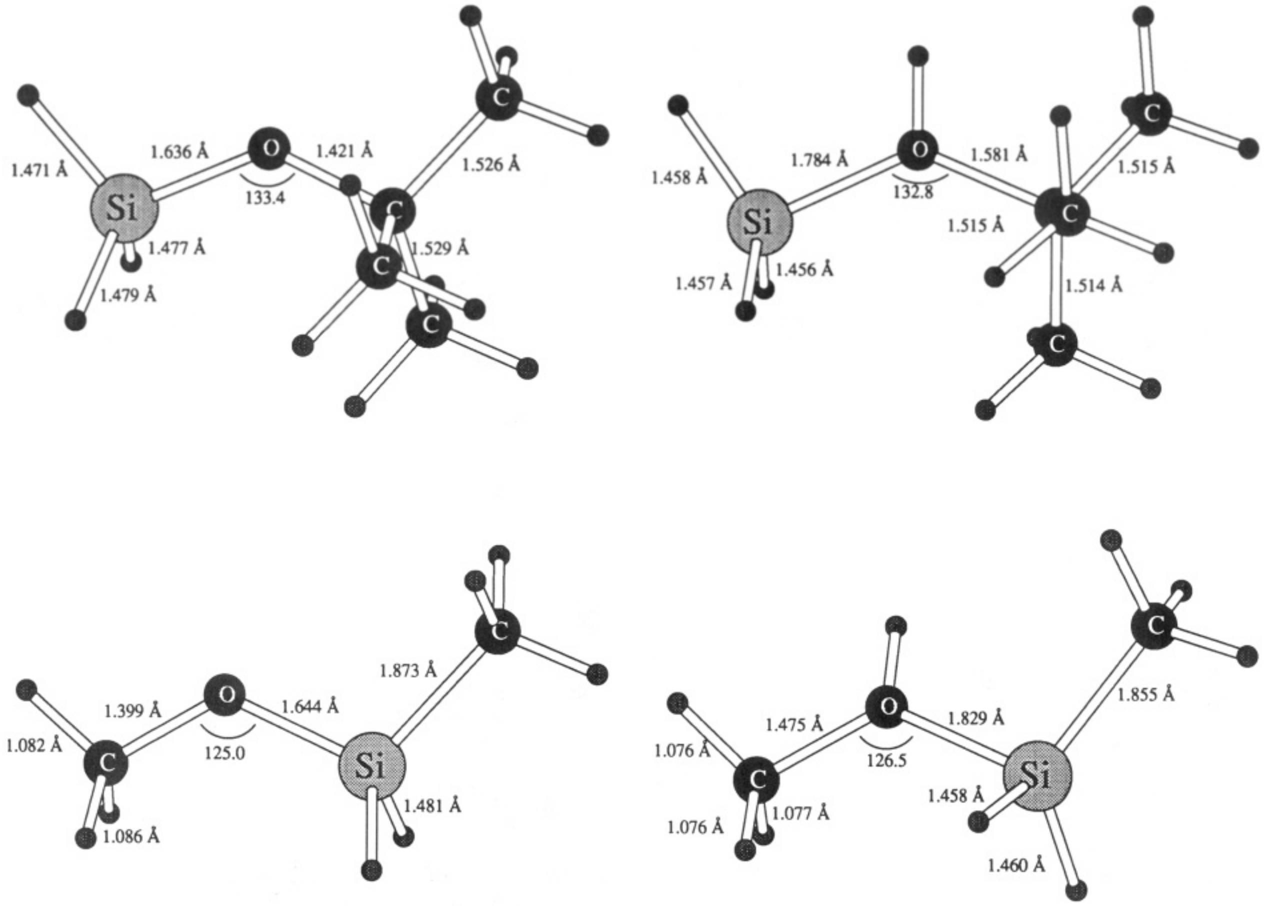

Figure 3. Optimized structures for *tert*-butyl silyl ether (top) and methyl methylsilyl ether (bottom) from 6-31G(d) calculations.

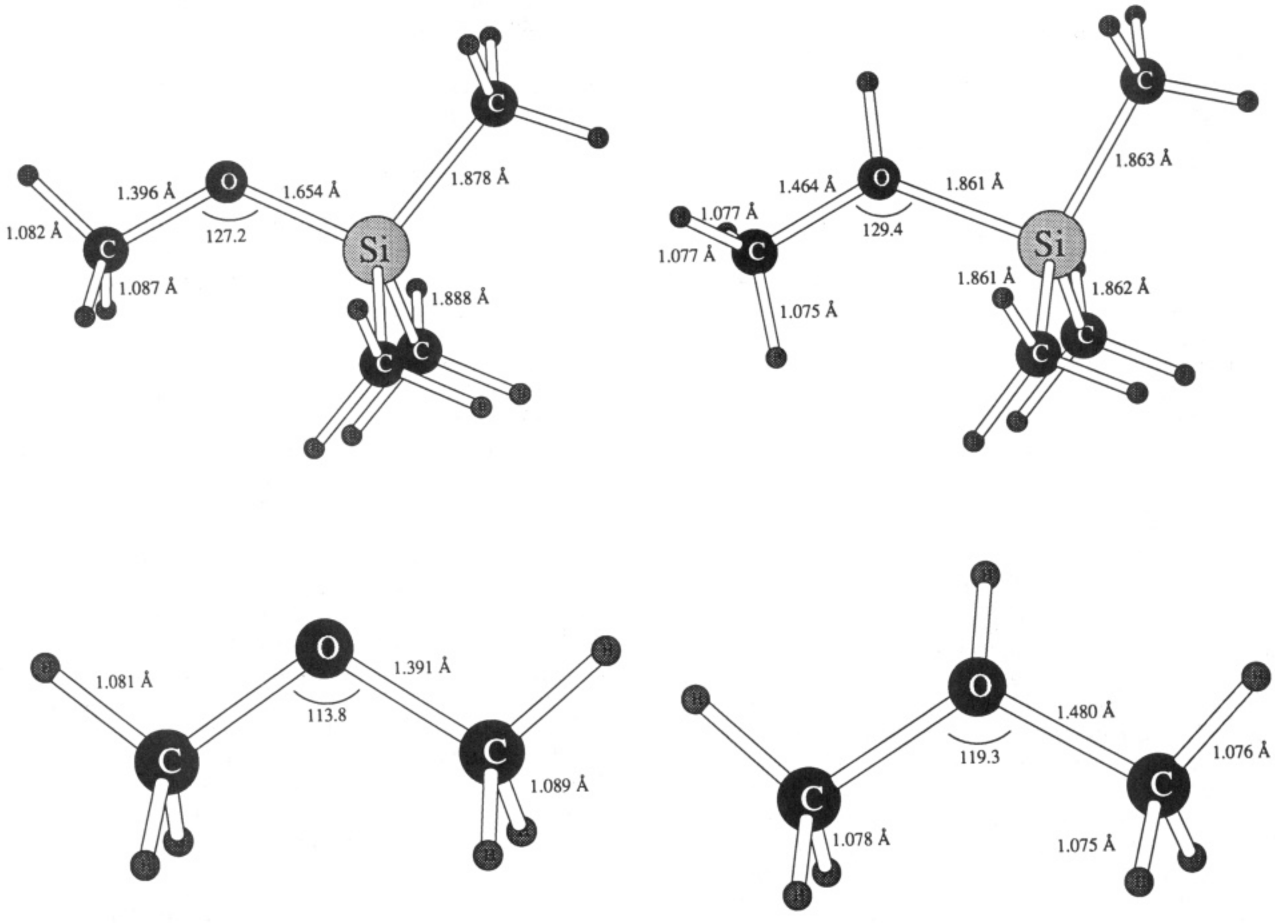

Figure 4. Optimized structures for methyl trimethylsilyl ether (top) and dimethyl ether (bottom) from 6-31G(d) calculations.

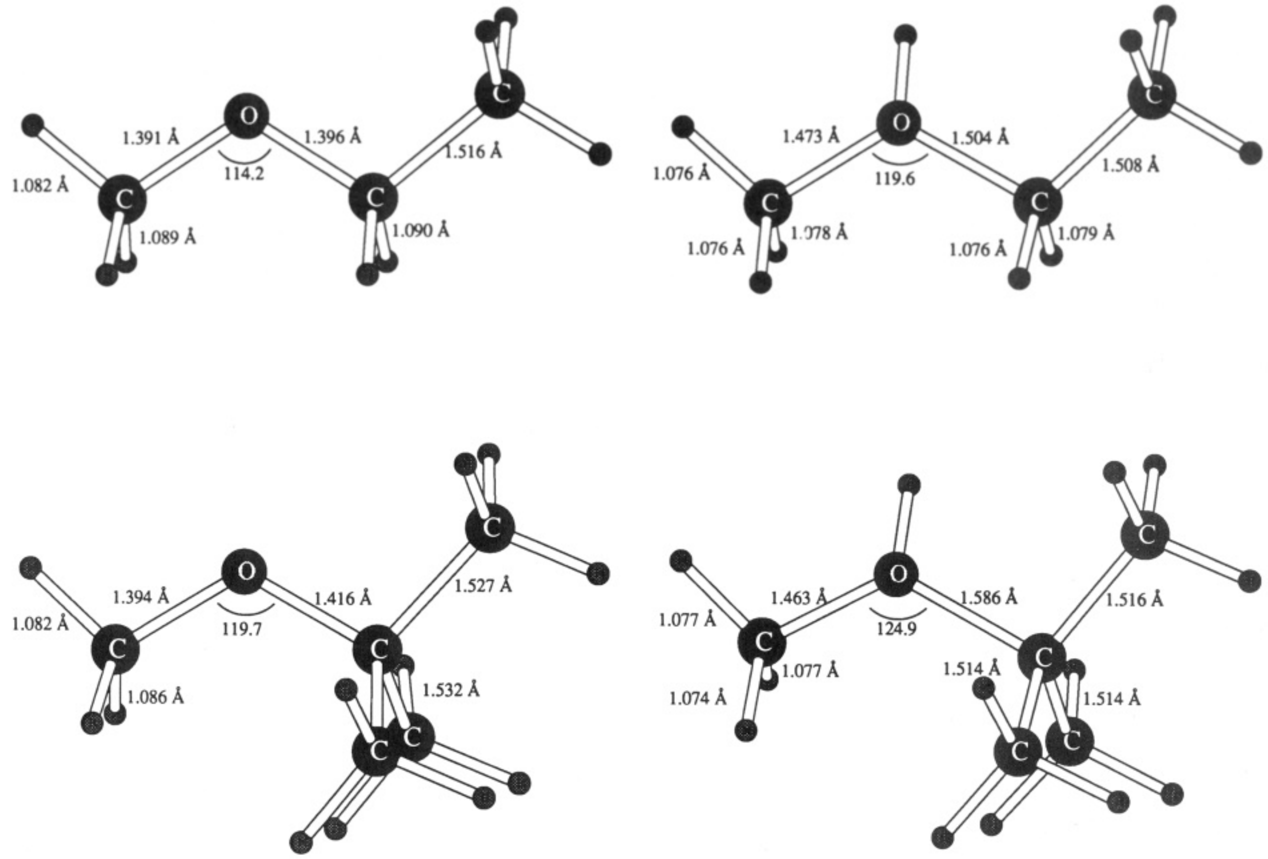

Figure 5. Optimized structures for ethyl methyl ether (top) and *tert*-butyl methyl ether (bottom) from 6-31G(d) calculations.

to the other alkyl silyl ethers, MTMSE registers the largest C–O–Si bond angle increase upon protonation (2.2°). MTMSE also has the greatest O–Si bond length increase (0.207 Å) and the smallest O–C increase (0.068 Å). These effects are consistent with a significant contribution from a methanol–trimethylsilylenium ion resonance structure.

For purposes of comparison, dimethyl ether (DME), ethyl methyl ether (EME), and *tert*-butyl methyl ether (TBME) were also considered. The computed geometry for DME agrees well with a microwave structure that found r(C–O) = 1.410 Å, r(C–H, in plane) = 1.091 Å, r(C–H, out-of-plane) = 1.100 Å, and ∠ C–O–C = 111.7°.[29] Upon protonation, dimethyl ether undergoes the most dramatic increase in its central bond angle in comparison to the other simple ethers. The 5.5° increase in the C–O–C angle is accompanied by an increase in the O–C distance of 0.089 Å. For ethyl methyl ether (Figure 5) an experimental geometry is also available.[30] The gas-phase microwave study found r(C–C) = 1.520 Å, r(H_3C–O) = 1.415 Å, r(CH_3CH_2–O) = 1.404 Å, and ∠ C–O–C = 111.8°. It was also determined that the s-trans conformer predominates, consistent with prior ab initio studies.[1,18,31] Comparing the geometrical parameters, it is clear that the 6-31G(d) level of theory consistently overestimates the C–O–C angles by 2–3° and underestimates O–C bond lengths by ca. 0.02 Å.[17] The computed structure of protonated ethyl methyl ether reveals the expected increases in the O–CH_3 (0.082 Å) and O–CH_2CH_3 (0.108 Å) distances and decrease in the C–C bond length (0.008 Å), accompanied by an increase of 5.4° for the C–O–C angle. The results for TBME in Figure 5 complete the series. Consistent with some steric repulsion between the alkyl groups, the O–C bonds are longer than in either DME or EME and the C–O–C angle widens to 119.7°. Upon protonation, the C–O–C angle increases by 5.2°, while the O–CH_3 and O–$C(CH_3)_3$ bonds lengthen by 0.069 and 0.170 Å. Clearly, a greater contribution from the resonance structure with the charge on the *tert*-butyl group is indicated.

Inspection of the preceding results reveals additional trends. In each of the three classes of ethers studied (alkyl, alkyl silyl, and disilyl), generalizations may be made regarding the effects of increasing alkyl substitution and protonation on the geometrical parameters. For example, for the series dimethyl, ethyl methyl, TBME, protonation leads to increased O–CH_3 distances. However, as the size of the other alkyl group increases, the increases in the O–CH_3 distance become smaller (i.e., Δr(O–CH_3) = 0.089, 0.082, and 0.069 Å, respectively). The opposite effect is noted for the other O–C bond, with the length increase becoming larger (i.e., Δr(O–CR_3) = 0.089, 0.108, 0.170 Å). These effects can be attributed to diminishing contributions from the less stable resonance structure with the charge on the methyl group and increasing contributions from the alternative with the charge on the methyl group and increasing contributions from the alternative with the charge on the larger alkyl group. The same trend is exhibited in the alkyl silyl ethers. Upon going from methoxysilane to methylsilyl methyl ether to MTMSE, the increase in O–CH_3 bond length becomes smaller (i.e., Δr(O–CH_3) = 0.080, 0.076, and 0.068 Å, respectively). Similarly, the O–Si length increase becomes larger (i.e., Δr(O–Si) = 0.174, 0.185, and 0.207 Å, respectively). Though only two disilyl ethers are available for comparison, the above trend holds. The lengthening of the O–SiH_3 bond distances in disiloxane and methyl disiloxane are 0.183 and 0.173 Å, respectively.

---

(29) Blukis, U.; Kasai, P. H.; Meyers, R. J. *J. Chem. Phys.* **1963**, *38*, 2753.

(30) Hayashi, M.; Kuwada, K. *J. Mol. Struct.* **1975**, *28*, 147.

(31) Jorgensen, W. L.; Ibrahim, M. *J. Am. Chem. Soc.* **1981**, *103*, 3976. Grigoras, S.; Lane, T. H. *J. Comput. Chem.* **1988**, *9*, 25.

Table II. Computed Thermodynamic Quantities[a]

species	ΔE_0^{elec}	ΔE_0^{vib}	$\Delta(\Delta E_{298}^{\text{vib}})$	ΔH_{298}	$T\Delta S_{298}$[b]	ΔG_{298}	ΔH_{298} exptl[c]
$(SiH_3)_2O$	−191.8	5.5	0.6	−187.1	−5.6	−181.5	
$H_3SiOSiH_2CH_3$	−196.2	6.3	0.4	−191.0	−6.9	−184.1	
H_3SiOCH_3	−197.1	6.6	0.4	−191.5	−6.8	−184.7	
$(CH_3)_2O$	−197.1	7.0	0.4	−191.3	−6.0	−185.3	−192.1
$H_3SiOC_2H_5$	−200.2	6.6	0.4	−194.7	−6.7	−188.0	
$H_3COC_2H_5$	−201.0	6.8	0.4	−195.3	−6.5	−188.9	−196.4
$H_3COSiH_2CH_3$	−202.1	6.7	0.4	−196.5	−7.0	−189.5	
$H_3SiOC(CH_3)_3$	−206.0	6.6	0.4	−200.5	−7.7	−192.8	
$H_3COSi(CH_3)_3$	−210.3	6.7	0.3	−204.6	−6.9	−197.7	−203
$H_3COC(CH_3)_3$	−210.6	6.7	0.4	−205.0	−6.5	−198.5	−202.2

[a] Frequencies computed using 3-21G optimized geometries; all values in kcal mol^{-1}. ΔE_0^{elec} is the MP3/MP2/6-31G(d)//6-31G(d) energy change. [b] $S_{298}(H^+) = 26.0387 \pm 0.005$ cal K^{-1} mol^{-1}.[33] [c] Experimental values from ref 7.

While the neutral species display similar geometries among analogous silyl- and methyl-substituted compounds, the protonated forms show important qualitative differences. One observation concerns the degree of pyramidilization at oxygen. In the series Si–O–Si, C–O–Si, and C–O–C, the calculated extents of nonplanarity range from 0 to 3°, 8 to 16°, and 41 to 43°, respectively. The planarity of the Si–O(H)–Si$^+$ framework has been documented in previous studies.[18] Furthermore, the general trend is consistent with the usual pattern of decreasing inversion barriers for XY_3 molecules as the electronegativity of Y decreases.[32] It should also be noted that there is often significant rotation of the substituent groups upon protonation as illustrated in Figures 1–5. For the silyl ethers, the alkyl groups rotate more than the silyl groups. The former are likely more sensitive to the presence of the added proton on oxygen in view of the shorter C–O than Si–O bonds.

Proton Affinities. The proton affinity (PA) of a molecule B is defined as $-\Delta H_{298}$ for eq 1. The computed

$$B + H^+ \rightarrow BH^+ \qquad (1)$$

proton affinities and gas-phase basicities (ΔG_{298}) are recorded in Table II in addition to the energetic terms obtained from the vibrational analyses. These are the change in zero-point energy (ΔE_0^{vib}) and the vibrational energy change between 0 and 298 K ($\Delta(\Delta E_{298}^{\text{vib}})$). The enthalpy change at 298 K relative to the reactants (ΔH_{298}) was computed via eq 2 where ΔE_0^{elec} is the electronic energy change at the MP3/6-31G(d)//6-31G(d) level. The re-

$$\Delta H_{298} = \Delta E_0^{\text{elec}} + \Delta E_0^{\text{vib}} + \Delta(\Delta E_{298}^{\text{vib}}) + \Delta E_{298}^{\text{rot}} + \Delta E_{298}^{\text{trans}} + \Delta(PV) \qquad (2)$$

maining terms represent the changes in the rotational and translational energy and the work term, which together contribute $-5/2RT$ (assuming ideal gas behavior). The entropy and free energy changes were likewise computed from standard formulas.[17]

Incorporating the vibrational energies and thermal corrections gives rise to modest decreases in the computed proton affinities (Table II). As expected,[1] disiloxane is computed to have the lowest PA (187.1 kcal mol^{-1}). It also possesses the lowest zero-point energy and greatest $\Delta(\Delta E_{298}^{\text{vib}})$, indicative of the flexible Si–O–Si backbone and weaker O–Si bonds. The present computed PA is significantly lower than the 201.1 kcal mol^{-1} calculated by Glidwell and Thomson at the 3-21G level.[18a] Methylation of disiloxane increases the computed PA by 3.9 kcal mol^{-1}. This increase is consistent with observations for analogous ethers.[6,7] Using the data in Tables I and II, one can confirm the importance of using extended basis sets and including correlation energy corrections. For all compounds considered, the 3-21G results are an average of 14.2 kcal mol^{-1} higher than the values of ΔE_0^{elec} listed in Table II. The 6-31G(d) results are on average 13.8 kcal mol^{-1} lower than the 3-21G predictions. The MP2 correction accounts for an additional 3.0 kcal mol^{-1}, while the MP3 correction subtracts 2.6 kcal mol^{-1}.

Methoxysilane and dimethyl ether are computed to have nearly identical PA's. While the computed PA of methoxysilane is actually 0.2 kcal mol^{-1} higher, the calculated gas-phase basicity of dimethyl ether is greater by 0.6 kcal mol^{-1}. The computed and observed PA's for dimethyl ether are in excellent agreement (191.3 vs 192.1 kcal mol^{-1}). As stated earlier, the silyl ether database is mostly qualitative; in contrast, the proton affinities of several dialkyl ethers are firmly established.[7]

In an analogous comparison, the computed PA's of ethoxysilane and ethyl methyl ether now favor the dialkyl ether by 0.6 kcal mol^{-1}. Compared to the experimental value (196.4 kcal mol^{-1}), the computed PA of ethyl methyl ether (195.3 kcal mol^{-1}) is 1.1 kcal mol^{-1} too low. However, the computed relative PA's of dimethyl ether and ethyl methyl ether are within 0.3 kcal mol^{-1} of the observed value (4.0 vs 4.3 kcal mol^{-1}).[7] Interestingly, methyl methylsilyl ether is calculated to have a PA 1.8 kcal mol^{-1} greater than its isomer, ethoxysilane, and 1.2 kcal mol^{-1} greater than ethyl methyl ether. Though the differences are small, the latter result violates the general notion that replacement of Si by C should increase the PA. The final three PA's computed (TBSE, MTMSE, and TBME) return to the conventional trend for replacement of silicon by carbon. Comparison of the computed PA's of MTMSE and TBME reveals a difference of only 0.4 kcal mol^{-1}, highlighting again the similarities in PA's between equivalent alkyl and alkyl silyl ethers. The experimental estimate of the PA of MTMSE (203 kcal mol^{-1})[7] and the computed value (204.6 kcal mol^{-1}) are in good accord. For comparison, Li and Stone report the PA(HMDS) = 203.4 kcal mol^{-1} and PA$(((CH_3)_3C)_2O)$ > PA(HMDS).[10] Finally, the discrepancy between theory (205.0 kcal mol^{-1}) and experiment (202.2 kcal mol^{-1}) approaches 3 kcal mol^{-1} for TBME. On the basis of higher level calculations on smaller molecules,[17,19,20] adding p-type polarization functions on hydrogens would raise the proton affinities by several kcal mol^{-1} and further extensions of the basis set to the Hartree–Fock limit would lower them back near the 6-31G(d) values. At all extended basis set levels, enhancement of the correlation energy calculations from the MP3 to MP4 level has little (<1 kcal mol^{-1}) effect on computed proton affinities.[19,20]

Looking at the computed results as a whole reveals some notable patterns. (1) For all ethers (disilyl, alkyl silyl, and

---

(32) Mislow, K. *Trans. N. Y. Acad. Sci.* **1973**, *35*, 227. Lehn, J.-M. *Top. Curr. Chem.* **1970**, *15*, 311.

(33) Chase, M. W., Jr.; Davies, C. A.; Downey, J. R., Jr.; Frurip, D. J.; McDonald, R. A.; Syverud, A. N. *J. Phys. Chem. Ref. Data* **1985**, *14*, S1.

dialkyl), increasing alkylation increases the PA's. (2) For disilyl ethers, replacement of a silicon by carbon increases the PA by 3–6 kcal mol^{-1}. (3) For alkyl silyl ethers, replacement of the silicon by carbon leads to variable effects on the PA. For isomers H_3COSiR_3 and H_3SiOCR_3, the methyl ethers have the higher PA's. (4) For methyl ethers, CH_3OY, PA's decrease along the series Y = $(CH_3)_3C \approx (CH_3)_3Si > CH_3SiH_2 > CH_3CH_2 > CH_3 \approx SiH_3$. This substituent order is consistent with the gas-phase observations of Pitt et al., namely, $(CH_3)_3C \geq (CH_3)_2CH \geq (CH_3)_3Si \geq (CH_3)_2SiH \geq CH_3CH_2 > CH_3 > H$.[6] The most surprising result here is the general similarity between the gas-phase proton affinities for alkyl silyl ethers and analogous dialkyl ethers.

A final observation may be made regarding the computed entropy terms. Both disiloxane and dimethyl ether possess comparatively more positive entropy changes upon protonation. These results partially from the fact that both molecules possess C_{2v} symmetry and, upon protonation, experience less rotational entropy loss than their lower symmetry counterparts, equivalent to $R \ln 2$ or ca. 0.4 kcal mol^{-1}.[34] Inspection of the individual entropy contributions confirms that both methyl ether and disiloxane have lower rotational entropies. However, the bulk of the entropy loss is accounted for by the change in translational entropy upon protonation.

Conclusion

The results presented in this paper document the geometrical and energetic changes that occur for the gas-phase protonation reactions of a series of alkyl and silyl ethers. The general trend among the alkyl ethers upon protonation is toward lengthening of the O–CR_3 and O–CH_3 bonds by roughly 0.14 and 0.08 Å, respectively, and widening the C–O–C angle by ca. 5°. The silyl ethers display similar trends, with more pronounced O–SiR_3 bond lengthening of 0.170–0.20 Å and Si–O–C angle widening of ca. 2°.

Correlation energy corrections and vibrational energy terms are needed for the reliable computation of absolute gas-phase proton affinities and basicities. The accord with the available experimental data suggest that the predicted thermodynamic results are within 3 kcal mol^{-1} of the true values. The low gas-phase basicity of disiloxanes has been confirmed, while the similar gas-phase basicity for dialkyl ethers and analogous alkyl silyl ethers has also been quantified.

Acknowledgment. Gratitude is expressed to the National Science Foundation for support of this work and to Scott G. Wierschke for computational assistance.

Supplementary Material Available: Detailed results of the 6-31G(d) geometry optimizations for the molecules in Figures 1–5 in Gaussian archive formate (6 pages). Ordering information is given on any current masthead page.

---

(34) Bailey, W. F.; Monahan, A. S. *J. Chem. Educ.* 1978, 55, 489.

Supersonic Jet Studies of Ethoxybenzenes: Geometry of Their Minimum Energy Conformations

E. R. Bernstein,* Hoong-Sun Im, and Mark A. Young†

Department of Chemistry, Condensed Matter Sciences Laboratory, Colorado State University, Fort Collins, Colorado 80523

Henry V. Secor, Ronald L. Bassfield, and Jeffrey I. Seeman*

Phillip Morris Research Center, P.O. Box 26583, Richmond, Virginia 23261

Received February 13, 1991

Supersonic jet mass resolved excitation spectroscopy and MOPAC 5/AM1 calculations are employed to demonstrate that the minimum energy conformation of ethoxybenzene and a number of its ortho-unsubstituted (i.e., sterically unhindered) derivatives is the planar form for which $\tau_1(C_{ortho}–C_{ipso}–O–C_\beta) = 0°$ and $\tau_2(C_{ipso}–O–C_\beta–C_\gamma) = 180°$. For 1-ethoxy-3-methylbenzene, two spectroscopic origin transitions are observed, one each for the conformations in which the $C_\beta H_2–C_\gamma H_3$ fragment is syn and anti to the C(3)-methyl substituent. For 1-ethoxy-4-ethylbenzene, a single origin transition is observed, as demonstrated by examination of two deuteriated derivatives.

Introduction

Aromatic compounds possessing alkyl or heteroalkyl substituents are ubiquitous in nature and play an important role in organic chemistry as a whole. Conformational analysis of these substances continues to receive intense attention,[1] in part because the literature frequently contains conflicting conclusions regarding the geometry of the minimum energy conformations of specific substituents.[2] A case in point is the aromatic ethoxy substituent, for which ethoxybenzene (phenetole, 1) is the prototype. On the basis of room-temperature IR data, the all (heavy

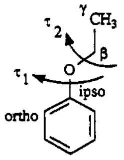

1

$\tau_1 = \tau(C_{ortho}–C_{ipso}–O–C_\beta)$
$\tau_2 = \tau(C_{ipso}–O–C_\beta–C_\gamma)$

[†] Present address: Department of Chemistry, University of Iowa, Iowa City, IA 52242.

0022-3263/91/1956-6059$02.50/0